JOURNAL OF MATERIALS SCIENCE **40** (2005) 1967–1974

Determination of essential work of fracture in EPBC sheets obtained by different transformation processes

J. GÁMEZ-PÉREZ, P. MUÑOZ, J. I. VELASCO, A. B. MARTÍNEZ, M. LL. MASPOCH*
Centre Català del Plàstic, Universitat Politècnica de Catalunya (UPC), Colom 114, Terrassa 08222, Spain
E-mail: maria.lluisa.maspoch@upc.es

1 mm sheets of polypropylene and ethylene-propylene block copolymers (EPBC) have been obtained using different processing methods in order to study the influence of processing induced morphology in the fracture properties of these materials. The processing methods employed were compression moulding (CM), extrusion-calendering (EC) and injection moulding (IM). Additionally, the sheets obtained by extrusion and injection were submitted to an annealing process with the aim to obtain more homogeneous morphologies that would ease their characterization.

The morphology has been characterized by different techniques: Polarizing light microscopy (MLP), differential scanning calorimetry (DSC), wide-angle X-ray diffraction scattering (WAXS) and scanning electron microscopy (SEM).

The fracture properties were determined by the essential work of fracture (EWF) method for deeply double edge notched specimens (DDENT), since these materials show ductile and post-yielding fracture behaviour. The EWF technique was applied in both the melt flow (MD) and the transversal (TD) directions in the sheets obtained by extrusion and injection moulding.

Results show that the sensitivity of the technique allows examining the effect of morphological variations of thin sheets, as well as a better characterization of the orientation level (versus other parameters like yielding stress or elastic modulus obtained by tensile test).

1. Introduction

The use of Ethylene-Propylene Block Copolymers (EPBC) is nowadays being increased in plastic industries. Melting and glass-transition temperatures are higher for polypropylene than for polyethylene. For this reason, EPBC can be used in a wider range of temperatures than polypropylene and polyethylene homopolymers. EPBC have a good mechanical resistance above the glass-transition temperature of polyethylene and a good behaviour under stress below the melting temperature of polypropylene. This combination allows the EPBC to be used in a wide range of common items, from packaging to automobile industries.

Polyolefins are in general semi crystalline polymers, whose structure and final morphology are not only depending on chain distribution and chemical disposition, but also on the thermal history and moulding conditions, which strongly affect the structure of the final specimens. In order to show an example, Young's modulus of about 100 GPa has been found for an oriented film of polyethylene [1] while the same parameter for commercial polyethylenes is commonly reported between 0.8 and 2.2 GPa [2]. This difference reveals the influence that the transformation process may have on the final behaviour of a specimen and it has to be seriously considered.

Four different materials based on polypropylene have been studied and three different transformation processes have been used to obtain the sheets: compression moulding (CM), injection moulding (IM) and extrusion-calendering (EC). The relationship between microstructure changes and fracture behaviour has been studied in EPBC sheets of 1 mm thick.

The processing generates different microstructures that affect the fracture behaviour. The microstructures have been previously characterized using different techniques: DSC, PLM and WAXS [3]. The fracture behaviour has been analysed by means of the Essential Work of Fracture technique, using the method previously reported (EWF) [4–7].

*Author to whom all correspondence should be addressed.

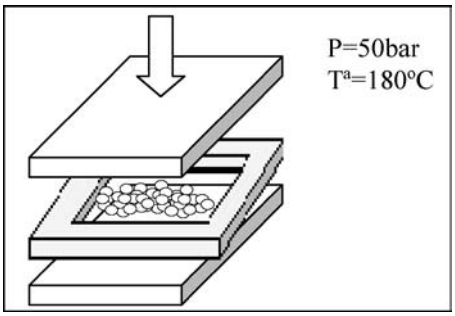

Figure 1 Scheme of Compression moulding process for (150 × 150 mm) sheets obtained from row material in pellets.

2. Materials and specimens

Four materials based on polypropylene have been used, a homopolymer (H0) and three EPBC with different ethylene content (5.5, 7.4. and 12.0) named C1, C2 and C3 respectively. The average weight percentage was determined by FT-IR spectroscopy [6]. All of them were kindly supplied by Bassell© in pellets form.

All materials used in this study have already been the topic of many other works of this research group. Therefore, a large quantity of information about these materials can be found in several articles and their references. A previous work carried out by our group [4], showed a great influence of an annealing treatment on the mechanical and fracture behaviour of films made of this materials. For such a reason, we consider interesting to complete the recently reported study for not-annealed injected plaques [7] with data of annealed ones. Furthermore, this work includes two other transformation processes: extrusion-calendering and compression moulding to have an overview of the influence that the transformation process have on the fracture behaviour.

Sheets of about 1 mm thick were obtained for all materials by different transformation processes as shown in Figs 1–3, in which the main process conditions are indicated.

Sheets obtained by extrusion-calendering and injection-moulding were submitted to a thermal treatment of annealing during 2.5 h at 130°C with the aim to obtain more homogeneous morphologies.

Two sorts of specimens were obtained from the sheets: Deeply Double Edge Notched Tensile (DDENT) specimens for Essential Work of Fracture analyses and normalized dumbbell specimens (ASTM-D638, type IV) for tensile tests.

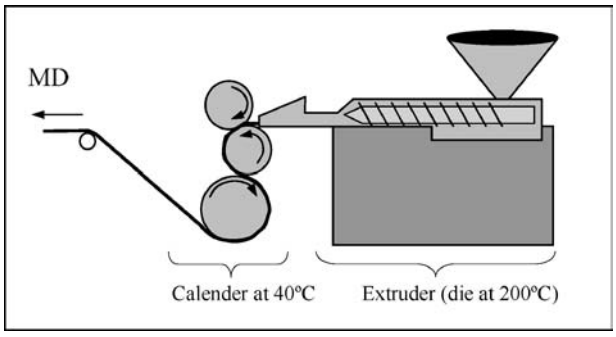

Figure 2 Scheme of the extrusion-calendering process for 100 mm-wide films.

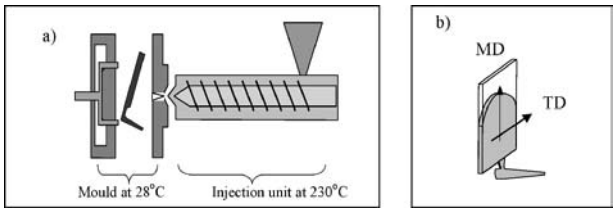

Figure 3 Schemes of injection-moulding process (a) and injected sheet of 100 × 100 mm (b).

3. Experimental methods

3.1. Morphological characterization

Morphology and microstructure characterization for all sheets was performed by Polarized Light Microscopy (PLM) and Differential Scanning Calorimetry (DSC). Wide Angle X-ray Diffraction Spectroscopy (WAXS) and Scanning Electron Microscopy (SEM) completed the analyses in some of the cases to aid in a better understanding of the EWF results.

Slices of about 20 μm thick were cut from the central part of EPBC sheets using a microtome (Reichert Jung 2040). The samples were observed with a polarizing light microscope magnifying at 40×. In semicrystalline polymers, the skin/core structure can be observed with the aid of polarized light since both microstructures show different birefringence [8].

DSC tests were carried out using a Perkin Elmer Pyris 1 series calorimeter to characterize the morphology of the skin and core zones. Samples from 10 to 15 mg were cut from skin and core separately and heated from 30 to 200°C at 10°C/min in aluminium pans. The melting enthalpies, ΔH_f were obtained from the recorded DSC thermograms (heat flow versus temperature curves).

WAXS experiments were performed on a Siemens D5000 Twin diffractometer with a radiation source of (40 kV, 30 mA).

More details of these experimental methods can be found in previous studies of our group [3, 5, 7] .

3.2. Mechanical and fracture characterization

It is well known that both injection-moulding and extrusion-calendering processes can induce orientation. Therefore, for the tensile tests and fracture analyses, the two main directions were considered: melt flow direction (MD) and transversal direction (TD).

Young's Modulus, (E) and yielding stress, (σ_y) were determined by tension loading tests according to the ASTM-D638 procedure. They were performed on a Galdabini universal testing machine at 2 mm/min and room temperature (26°C).

The fracture behaviour has been studied by the EWF method. This technique was initially developed by Cotterell and Reddel [9] applying to metals the work of Broberg on ductile fracture [10]. Afterwards, it was applied to ductile polymers by Cotterell and Mai [11]. The theory postulates that under plane-stress state, the total energy (W_f) needed for the fracture of a DDENT specimen (Fig. 4) can be split into two terms (in a quasi-static crack propagation test). The two terms are: the

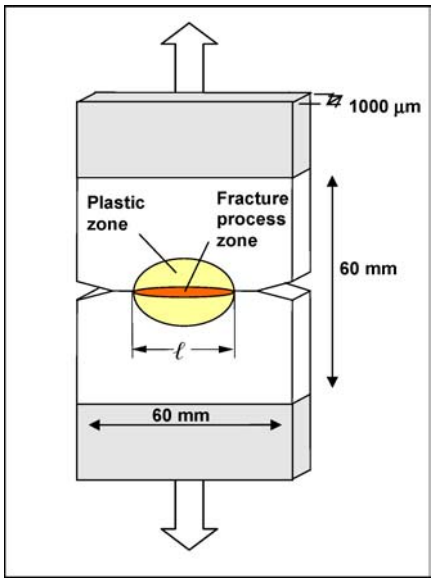

Figure 4 Geometry and dimension details of a DDENT fracture specimen.

essential work of fracture (W_e) and the non-essential work of fracture or plastic work (W_p).

The energy absorbed during the fracture is represented by W_e and it is proportional to the ligament section. On the other hand, W_p collects all other sources of dissipative work that occurs outside the fracture surfaces and it is proportional to the volume of the deformed zone, resulting the following expression:

$$W_f = W_e + W_p = w_e \ell\, t + w_p \beta \ell^2\, t \qquad (1)$$

Where the work of fracture has been expressed as a function of the specific essential work of fracture w_e and the non-essential specific work of fracture w_p. In (1), ℓ is the ligament length, t is the thickness and β is factor related to the geometry of the plastic zone.

The specific essential work of fracture, w_e can be easily determined by testing several specimens with different ℓ. W_f is obtained by numerical integration of its corresponding curve load-versus-displacement. After dividing the expression (1) by $(\ell \cdot t)$, the specific total work of fracture is obtained as a function of ℓ:

$$w_f = w_e + \beta w_p \ell \qquad (2)$$

Plotting this expression is easy to obtain the essential work of fracture value (w_e) as y-intercept and the plastic item (βw_p) by means of the slope.

The plane-stress essential work of fracture is a material constant only dependent on the thickness but not affected by the specimen geometry. At least, ten ligament lengths were tested among a valid testing ℓ-range from 5 to 15 mm, following the ESIS protocol for the EWF method [12].

Following the protocol, the precrack has been induced in DDENT specimens making a deep notch with a fresh razor blade at both sides of the specimen. The ligament length (ℓ) has been measured from post-mortem specimens, using a micrometer assembled to a travelling platform set on a Carlton binocular lens.

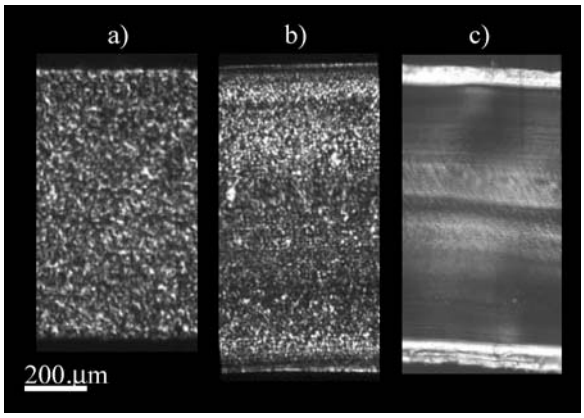

Figure 5 PLM microphotographs of 20 μm slices from H0 sheets and different processes: (a) CM, (b) EC and (c) IM.

4. Results and discussion

4.1. Morphological and micro structural analyses

PLM microphotographs from H0 slices of different processing sheets (Fig. 5) were obtained and revealed that:

- In compression moulding sheets, spherullites had a homogeneous size all along the thickness (Fig. 5a).
- Films obtained by extrusion-calendering showed variation of the spherullites size along the thickness. Smaller spherullites appeared in the skin while bigger ones were found in the core. (Fig. 5b).
- In sheets obtained by injection moulding, two different microstructures can be clearly appreciated (skin-core morphology). The relative thickness depends on the ethylene content, the thickness of the sheet and moulding temperature, among other parameters [3, 13] (Fig. 5c).

From PLM it has been found that similar microstructures for EPBC are obtained using different transformation processes, although the percentage of skin zone decreases when increasing the ethylene content [7].

In that work, it was shown that these microstructures are thermally stable at the temperature of annealing (130°C), since samples of annealed plaques did not reveal changes on their skin-core microstructure.

According to the thermograms obtained from Differential Scanning Calorimetry (DSC), it can be pointed out that:

- Melting enthalpies (see NA values in Table I) show that compression moulding process is able to develop a slightly higher crystallinity level than

TABLE I Melting enthalpies obtained from DSC analyses

	ΔH (J/g) IM- NA	ΔH (J/g) EC- NA	ΔH (J/g) CM	ΔH (J/g) IM-A	ΔH (J/g) EC-A
H0	112	127	127	133	138
C1	97	107	112	112	119
C2	86	96	111	94	107
C3	84	85	93	92	94

Note: NA—no annealing treatment.

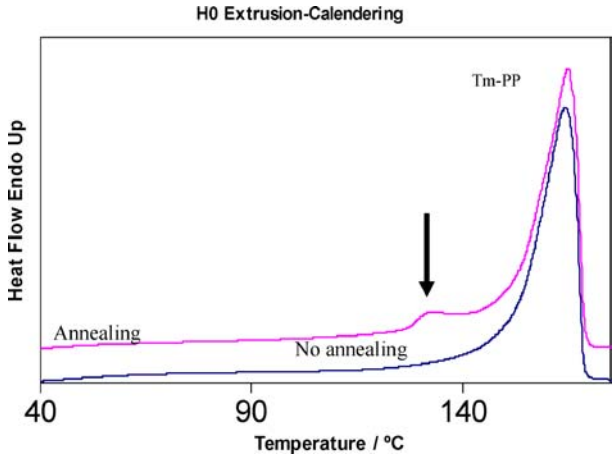

Figure 6 Thermograms of H0 samples obtained from Extrusion-Calendering sheets showing the reorganization of smectic phase (sm-PP) after annealing. Arrow in figure indicates the peak of the transition: sm-iPP $\rightarrow$ α-iPP during annealing.

injection moulding and extrusion calendering because the cooling process is slower.

- Injection moulding and extrusion-calendering sheets showed higher melting enthalpies after annealing than before being thermally treated (see A in Table I). This change in the EPBC morphology can be explained as an increasing of cristallinity due to a reorganization of the amorphous phase.
- DSC analyses for injection moulding and extrusion-calendering revealed significant amount of smectic phase of polypropylene, (sm-PP). Contrarily, this phase has not been found in compression moulding sheets as it could be expected due to its slow cooling process. The formation of sm-PP is commonly attributed to a high speed cooling [14]. Thermograms from H0 samples before and after annealing showed the existence of sm-PP as can be seen in Fig. 6 with the change of the curve shape. After annealing, a peak appears near the temperature in which the thermal treatment has been performed and is it attributable to the reorganization of the smectic phase [4].

The WAXS technique has been useful to study the skin-core microstructure of injection moulding sheets. The orientation of the skin zone has been measured by means of the A_{110} diffraction index of α-PP crystallites [15] and has been proved that the skin of the injection moulding sheets had higher orientation than the core of the same sheets [3]. Furthermore, WAXS analyses allowed to measure the β_{300} diffraction index, (related to the β-phase percentage). This showed the existence of β-PP only in the skin zone of injection moulding sheets. The existence of this phase is attributable to the combination of high shear stress and rapid cooling during the injection process. After annealing, a decreasing of β_{300} index has been found. This could be a consequence of an incorporation of some amorphous phase to α-PP crystallites, rather than the conversion of β-PP into α crystallites.

All these morphological and microstructure differences are based on the existence of shear and thermal gradient during cooling on the transformation process. During the injection, the melt is strongly submitted to shear stress when filling the mould at high flow speed, causing orientation of the polymer chains. Close to the mould surface, the combination of strong shear and high cooling rate causes the quenching of polymer chains, which promote oriented crystalline structures in the skin. Such microstructure has been studied by Fujiyama [8] using the shish-kebab-like model proposed by Keller and Machin [16]. On the other hand, the orientation of the core is lower than in the skin due to a slower cooling rate. For this reason, the final structure follows the Tadmor model [17], also known as skin-core.

In the extrusion-calendering process, the thickness of the film is shaped in the calender and the appearance of the film surface becomes smooth and flat. The film dimensions change during calendaring and this might induce slight orientation to the polymer chains. The melt flow of polymer material comes out through the extruder die and then goes through the calender rolls, which strain and shear the film in the melt flow direction at the same time it get cooled down. The quick cooling allows the formation of sm-PP. In addition, the gradient of temperatures between the surface and the internal part of the film produces a gradient of spherullites size, bigger in core than in skin due to a slower crystallization.

During the injection moulding process, the melt flow speed has been of about 10 m/min while the extrusion-calendering process has provided a much lower melt flow speed of about 1 m/min. Therefore, extruded films have been submitted to lower shear than injected sheets and this explains that extruded films had lower orientation and more homogeneous microstructure than injected sheets as can be deduced from PLM microphotography.

The crystalline morphology for compressed materials observed by means of PLM allowed us to deduce that no orientation has to be expected from sheets obtained by compression moulding since this transformation process has a very slow cooling rate at room temperature and provides lower shear to the material. So, the spherullites get a random disposition all along the thickness.

4.2. Fracture and mechanical characterization

Different fracture behaviours have been observed during the EWF test:

- *Post-yielding* fracture behaviour have been found for most of the materials tested in this study and consists of a ductile fracture with a fully yielded ligament prior to a stable crack propagation along the process zone (Fig. 7a).
- *Blunting* phenomena is characterized for having, after a fully yielded ligament, stable crack propagation with a strongly blunted crack tip [7] (Fig. 7b).
- When *necking* occurs, instead of a crack propagation perpendicular to the tensile direction, the

TABLE II Fracture parameters obtained by EWF for the four annealed materials: specific essential work of fracture, w_e and plastic item, βw_p

		Compression moulding		Extrusion calendering				Injection moulding			
				MD		TD		MD		TD	
H0	w_e (kJ/m^2)	Ductile		29.5	± 3.3	Ductile		[a]208	± 85	Brittle	
	βw_p (MJ/m^3)	instability		5.9	± 0.2	instability		[a]37	± 8	fracture	
C1	w_e (kJ/m^2)	36.1	± 3.5	[b]197	± 10.0	24.6	± 2.9	[a]250	± 40	20	± 2.0
	βw_p(MJ/m^3)	6.6	± 0.3	[b]14.4	± 0.8	5.0	± 0.2	[a]37	± 3	5.5	± 0.2
C2	w_e (kJ/m^2)	15	± 4.0	27.7	± 5.4	27.3	± 1.9	[b]91	± 10	19	± 1.0
	βw_p (MJ/m^3)	5.7	± 0.4	8.7	± 0.4	5.6	± 0.1	[b]18.1	± 1	3.4	± 0.1
C3	w_e (kJ/m^2)	5.9	± 1.5	30.9	± 3.3	21.1	± 1.1	41	± 2	14.6	± 0.7
	βw_p (MJ/m^3)	1.25	± 0.2	7.0	± 0.2	3.59	± 0.1	9.7	± 0.1	1.7	± 0.1

[a]Values corresponding to specimens with necking phenomenon.
[b]Values corresponding to specimens with blunting phenomenon.

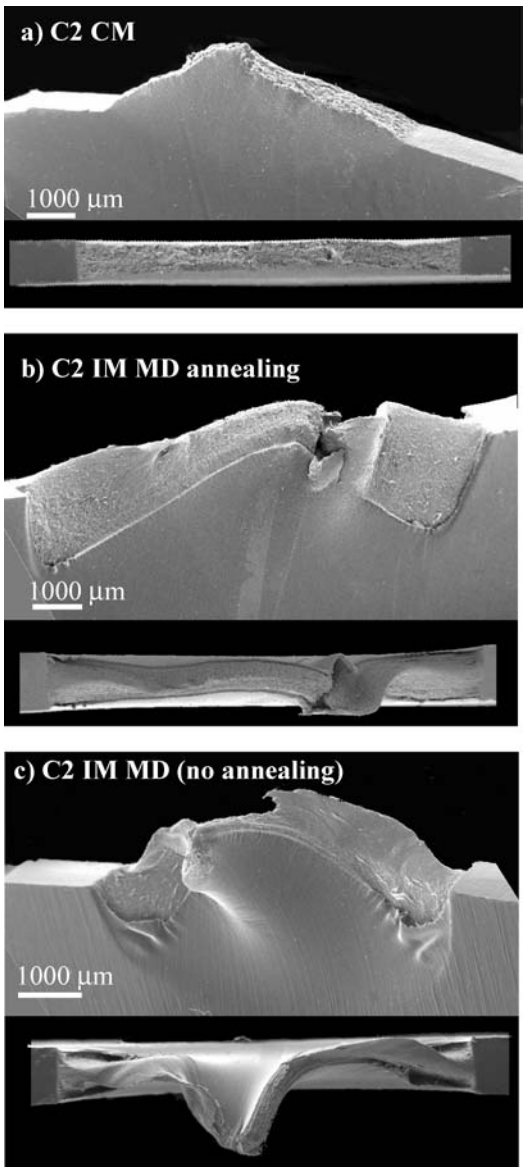

Figure 7 Scanning electron micrographs of fracture surfaces showing the three types of ductile fracture: post-yielding (a), blunting (b) and necking (c).

process zone yields with a high plastic deformation and the crack penetrates into the plastic zone [7] (Fig. 7c).

- *Brittle* behaviour can be observed for some H0 specimens tested in the transversal direction in which unstable crack propagation took place with no previous plastic deformation (Fig. 9a).
- *Ductile instability* is a fracture behaviour that can be found in polypropylene [4], which consists in initial ductile crack propagation under tension loading, followed by unstable crack propagation when the material reaches a critical stress value (Fig. 9b).

Although the EWF method can be applied to all ductile fracture cases, only those having post-yielding fracture (Fig. 7a) fulfill all EWF protocol requirements [12]. Therefore, all fracture parameters values shown in Table II corresponding to specimens with necking and blunting, have to be considered out of validity.

In Fig. 8, the load-displacement (L-dL) curves obtained for material C1 are shown as an example of the curves belonging to all valid cases. It is noticeable the accomplishment of the criterion of self-similarity for the L-dL curves. From these curves, the fracture parameters have been obtained following the EWF method.

A fractographic analysis performed by SEM revealed that:

- In specimens showing blunting and necking (Fig. 7b and c), a propagation of the crack out of the limits established in EWF theory occurs (outside of the ligament section). This phenomenon is, in both cases, able to absorb energy while the fracture process takes place as can be deduced from the comparison of w_f values, which are much higher than energies obtained when stable crack propagation occurs.
- H0 sheets obtained by injection moulding and tested in TD have shown patch patterns corresponding to crazing micromechanism (Fig. 9a). The formation of crazes perpendicular to the stress direction facilitates the propagation of the crack and finally drives the specimen to brittle crack propagation with no previous yielding. These patterns could not be observed in the cases where ductile instability fracture behaviour was found.
- Shear lips of plastic deformation, as a consequence of tearing [18], have shown differences depending on the testing direction, being clearer in MD than in TD.

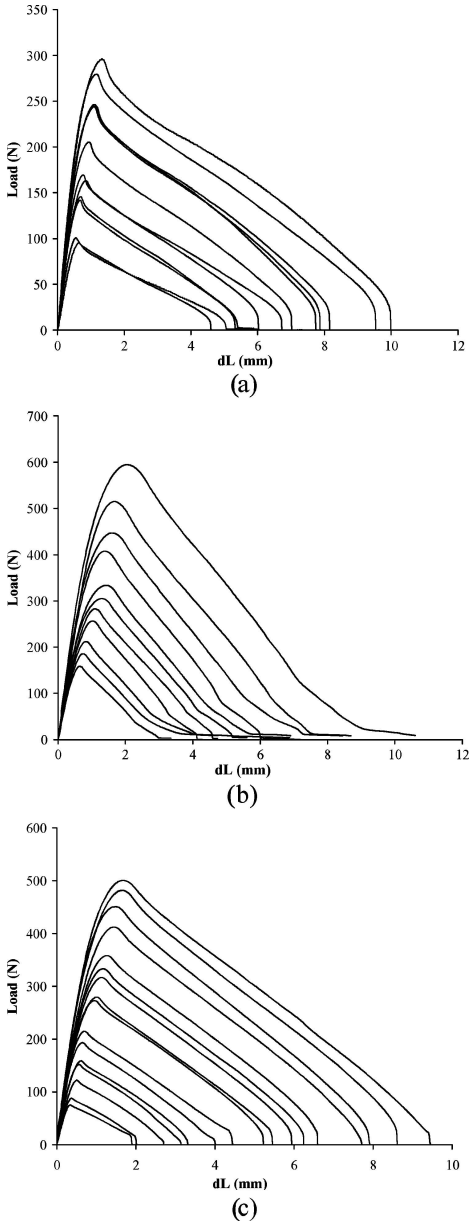

Figure 8 Curves load versus displacement for C1 specimens from annealed sheets obtained by Compression Molding (a); Injection Molding (b) and Extrusion Calendering (c). Ligament length ranges from 5 to 20 mm.

This phenomenon is less pronounced when the ethylene content increases as it has been proved by SEM (Fig. 10). Shear lips showing tearing plastic deformation can be appreciated in H0 (Fig. 10a), in contrast with the in-plane fracture in C3 (Fig. 10b).

A tendency has been also observed for the shape of the plastic region deformed by tearing depending on the process, being better-defined for processes which give more orientation to materials: IM > EC > CM.

Even considering that essential work of fracture and plastic item values are not strictly correct for those specimens that have shown necking and blunting, these can be qualitatively useful for tendency evaluations. Essential work of fracture values (w_e) for the three different transformation processes and two testing directions are plotted in Fig. 11, which shows that:

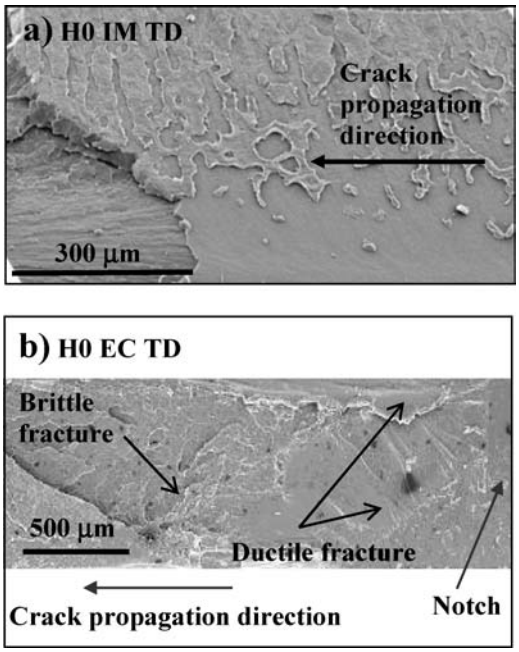

Figure 9 Scanning electron micrographs showing two types of brittle behaviour: Fragile fracture of a H0 IM TD specimen (a) and ductile instability phenomenon of a H0 EC TD specimen (b).

- w_e values obtained for MD are higher than TD values. These differences decrease when increasing the amount of ethylene. Therefore, it can be concluded that ethylene content decreases the processing induced orientation since the ethylene blocks contribute to a higher mobility of the polymer chains [7].
- The increase of ethylene content causes a decrease of toughness represented by w_e and βw_p parameters. This tendency is clear for compressed sheets and for MD specimens of materials obtained by injection moulding and extrusion-calendering. In TD direction, this tendency is not so clear but perceptible.

The deformation of the polyethylene blocks involves less energy than the deformation of the polypropylene blocks. At room temperature, PP blocks have no movement restrictions and they govern the plastic behaviour of the material [4, 7]. All this provides an explanation to the toughness tendencies found with the increase of EC.

The above mentioned observations are strongly related to the degree of orientation induced by the different transformation processes. Theoretically, fracture parameters such w_e and βw_p obtained for single-direction CM sheets should appear between those obtained from MD and TD specimens from extruded films and injected sheets. This is accomplished for the material C1, partially for C2 but not at all for C3 whose values were lower than its MD-TD range.

Although an explanation for this phenomenon is still to be found, it is supposed that a higher ethylene content is the main factor to be considered because of the influence that it may have on the resulting morphology.

H0 material deserves to be studied separately since EWF test revealed two types of phenomenon that avoided its analysis. Necking phenomenon occurred in

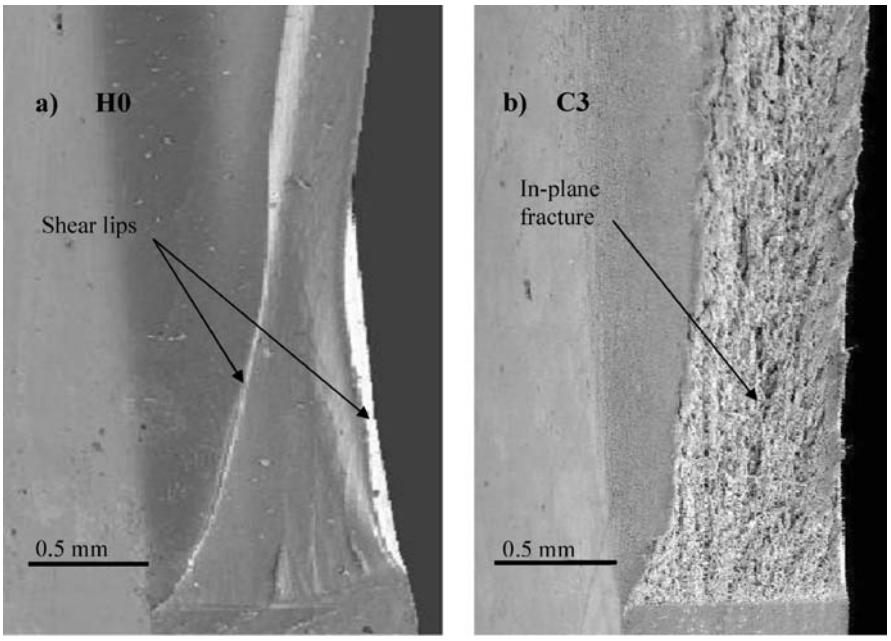

Figure 10 SEM photographs of H0 (a) and C3 (b) obtained by extrusion-calendering and tested in MD direction. Arrows in figures show shear lips (a) and in-plane fracture (b).

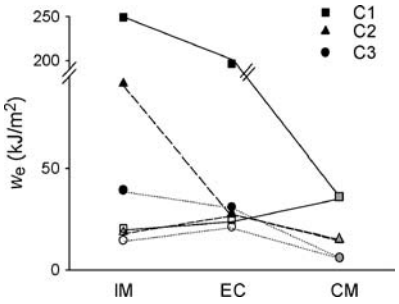

Figure 11 The influence of transformation processes on the essential work of fracture. (■-MD, □-TD).

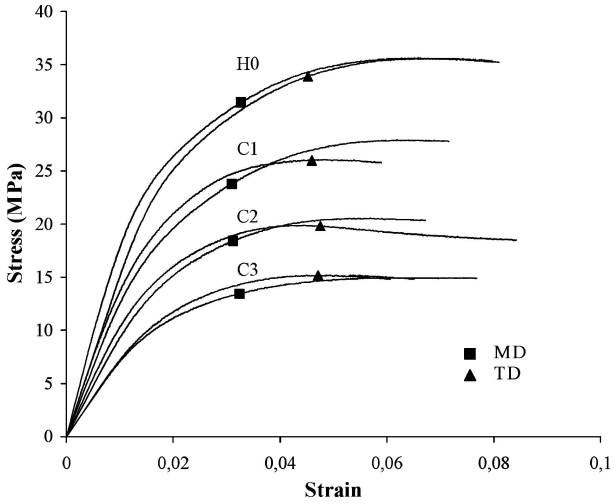

Figure 12 Stress versus strain curves obtained for all extruded materials (annealed) in both the MD and TD directions.

MD specimens of sheets obtained by injection moulding and extrusion-calendering and a global brittle behaviour was found for all specimens tested in TD: compression moulding and extrusion-calendering sheets showed ductile instability and injection sheets showed brittle fracture behaviour.

The different behaviour of materials is in concordance with the induced morphology caused by each process although only one of the tested materials, C3, can be analysed using the EWF with absolute validity.

The existence of a low ethylene content avoids the two brittle behaviours mentioned [4], allowing then the EWF analyses.

E and σ_y values (Table III) have been obtained from the stress-strain curves (Fig. 12). When analysing the mechanical behaviour of sheets, certain anisotropy for yielding stress, σ_y and Young's Modulus, E values can be observed. Differences for these tensile values due to orientation are less significant than for fracture parameters, and even less for those materials with low orientation.

On the other hand, when looking at the influence that the transformation process has on the mechanical behaviour (Table III), it can be proved that σ_y for MD specimens follow the same tendency than fracture parameters, w_e and βw_p. These parameters have lower values for compression moulding sheets than for extrusion-calendering sheets. The highest values for these parameters correspond to injection moulding process. For TD specimens, no common tendencies have been found for tensile and fracture parameters.

Calculated Young's Modulus show a tendency that does not depend on the testing direction. As a function of orientation levels, extrusion-calendering values should be comprised between CM and IM but the lowest E values have been found for extrusion-calendering sheets. However, the crystalline phase has to be taken as one of the factors that influence E values besides the induced orientation. The existence of sm-PP, generated during the extrusion-calendering transformation process, at high cooling rate, is the reason why E values are lower for extruded films than for sheets obtained by compression moulding.

TABLE III Mechanical parameters obtained by tensile measurements: yielding stress, σ_y and Young's Modulus, E. All values have been obtained after annealing

			Extrusion		Injection	
		Compression	MD	TD	MD	TD
H0	σ_y (MPa)	32.5 ± 1.4	35.6 ± 0.3	35.3 ± 0.2	40.5 ± 0.2	32.7 ± 0.2
	E (GPa)	1.86 ± 0.07	1.93 ± 0.04	1.52 ± 0.04	2.61 ± 0.08	2.19 ± 0.05
C1	σ_y (MPa)	25.2 ± 0.3	27.9 ± 0.3	25.1 ± 0.8	39.7 ± 0.4	27.7 ± 0.2
	E (GPa)	1.39 ± 0.04	1.27 ± 0.04	1.25 ± 0.05	1.98 ± 0.05	1.73 ± 0.02
C2	σ_y (MPa)	18.5 ± 0.9	20.0 ± 0.6	19.8 ± 0.3	29.5 ± 0.7	22.6 ± 0.2
	E (GPa)	1.33 ± 0.07	0.91 ± 0.02	0.91 ± 0.04	1.76 ± 0.04	1.55 ± 0.02
C3	σ_y (MPa)	11.9 ± 0.2	15.4 ± 0.4	14.9 ± 0.5	23.8 ± 0.23	18.7 ± 0.13
	E (GPa)	0.92 ± 0.03	0.75 ± 0.03	0.71 ± 0.04	1.55 ± 0.03	1.31 ± 0.03

All the above mentioned points out the convenience of an exhaustive morphology characterization in order to have a better comprehension of tensile and fracture behaviours of materials based on polypropylene.

5. Conclusions

The morphology of polymer sheets obtained from semi crystalline materials based on polypropylene is strongly dependent on the transformation process.

Fracture and tensile mechanical properties have shown morphology variations that reveal the strong dependence above mentioned. A remarkable anisotropy has been found for fracture and tensile parameters of both MD and TD principal testing directions.

EWF technique has been successfully performed in most of the material sheets to characterize the fracture of materials with two parameters (essential work of fracture and plastic item). More over, a higher sensibility than normal tensile tests has been proved for this technique in those cases whose orientation differences are hard to be found by normal tensile analyses.

Acknowledgments

The authors of this work deeply thank M. Marsal and his help provided for SEM photography acquirements as well as the economic support received from the 'Ministerio de Ciencia y Tecnología' through the MAT-2000-1112 project. J. Gamez-Perez thanks MCED for the concession of a pre-doctoral grant.

References

1. K. HIROFUMI, I. YOSHIMU, M. KAZUO, S. AKIRA and Y. SHIGEKI, European Patent 0376423 (1990).
2. W. HELLERICH, G. HARSCH and S. HAENLE, in "Guía de Materiales Plásticos," 5th ed. (Hanser, Barcelona, 1989).
3. M. L. MASPOCH, J. GÁMEZ-PÉREZ, E. GIMÉNEZ, O. O. SANTANA and A. GORDILLO, *J. Appl. Polym. Sci.* **93** (2004) 2866.
4. D. FERRER-BALAS, M. L. MASPOCH, A. B. MARTÍNEZ and O. O. SANTANA, *Polymer* **42** (2001) 1697.
5. D. FERRER-BALAS, M. L. MASPOCH, A. B. MARTÍNEZ, E. CHING, R. K. Y. LI and Y. W. MAI, *Polymer* 42(6) (2001) 2665.
6. D. FERRER-BALAS, in "Aplicación del método del Trabajo Esencial de Fractura para el estudio de films de polipropileno y copolímeros de polipropileno-polietileno en bloques," PhD Thesis Work (Technological University of Catalonia, 2001) p. 79.
7. M. L. MASPOCH, J. GAMEZ-PEREZ, A. GORDILLO, M. SÁNCHEZ-SOTO and J. I. VELASCO, *Polymer* **43** (2002) 4177.
8. M. FUJIYAMA, in "Higher Order Structure of Injection-Moulded Polypropylene in "Polypropylene, Structure and Morphology" (Chapman & Hall, London, 1995) p. 2739.
9. B. COTTERELL and J. K. REDDEL, *Int. J. Fract.* **13** (1977) 267.
10. K. B. BROBERG, *J. Mech. Phys. Solids* **23** (1975) 215.
11. B. COTTERELL AND Y. W. MAI, *Int. J. Fract.* **32** (1986) 105.
12. E. CLUTTON, in "Essential Work of Fracture in Fracture Mechanics Testing Methods for Polymers, Adhesives and Composites," edited by D. R. Moore, A. Pavan and J. G. Williams (Elsevier Science Ltd., Oxford, 2001) p. 177.
13. J. C. VIANA, A. M. CUNHA and N. BILLON, *Polymer* **43** (2002) 4185.
14. N. ALBEROLA, M. FUGIER, D. PETIT and B. FILLON, *J. Mater. Sci.* **30** (1995) 1187.
15. A. TURNER-JONES, J. M. AIZLEWOOD and D. R. BECKETT, *Macromol. Chem.* **75** (1964) 134.
16. A. KELLER and M. MACHIN, *J. Macromol. Sci.* **B1** (1967) 41.
17. Z. TADMOR, *J. App. Polym. Sci.* **18** (1974) 1753.
18. M. L. MASPOCH, D. FERRER-BALAS, A. GORDILLO and O. O. SANTANA, *ibid.* **73** (1999) 177.

Received 1 September
and accepted 16 December 2004